



UNIVERSITY OF LEEDS

This is a repository copy of *Subharmonic Plane Wave Imaging of Liposome-Loaded Microbubbles*.

White Rose Research Online URL for this paper:
<http://eprints.whiterose.ac.uk/143915/>

Version: Accepted Version

Proceedings Paper:

Nie, L orcid.org/0000-0002-5796-907X, McLaughlan, JR orcid.org/0000-0001-5795-4372, Cowell, DMJ et al. (2 more authors) (2018) Subharmonic Plane Wave Imaging of Liposome-Loaded Microbubbles. In: IEEE International Ultrasonics Symposium, IUS. 2018 IEEE International Ultrasonics Symposium, 22-25 Oct 2018, Kobe, Japan. IEEE .

<https://doi.org/10.1109/ULTSYM.2018.8580201>

Copyright © 2018, IEEE. This is an author produced version of a paper published in IEEE International Ultrasonics Symposium, IUS. Uploaded in accordance with the publisher's self-archiving policy.

Reuse

Items deposited in White Rose Research Online are protected by copyright, with all rights reserved unless indicated otherwise. They may be downloaded and/or printed for private study, or other acts as permitted by national copyright laws. The publisher or other rights holders may allow further reproduction and re-use of the full text version. This is indicated by the licence information on the White Rose Research Online record for the item.

Takedown

If you consider content in White Rose Research Online to be in breach of UK law, please notify us by emailing eprints@whiterose.ac.uk including the URL of the record and the reason for the withdrawal request.



eprints@whiterose.ac.uk
<https://eprints.whiterose.ac.uk/>

Subharmonic Plane Wave Imaging of Liposome-loaded Microbubbles

Luzhen Nie¹, James R. McLaughlan^{1,2}, David M. J. Cowell¹, Thomas M. Carpenter¹, and Steven Freear¹

¹Ultrasound Group, School of Electronic and Electrical Engineering, University of Leeds, Leeds LS2 9JT, U.K.

²Leeds Institute of Cancer and Pathology, University of Leeds, Leeds LS9 7TF, U.K.

E-mail: elln@leeds.ac.uk and s.freear@leeds.ac.uk

Abstract—A key component of targeted drug delivery using liposome-loaded microbubbles and ultrasound is the ability to track these drug vehicles in real time to guide payload release locally. As a uniquely identifiable emission from microbubbles, the subharmonic signal is of interest for this purpose. Acoustic characterization of liposome-loaded microbubble populations confirmed the decreased pressure threshold for subharmonic emissions (50 kPa vs. 200 kPa for normal microbubbles). This study proved the feasibility of subharmonic plane wave imaging of liposome-loaded microbubbles with improved subharmonic sensitivity especially at depth compared to their counterpart of bare (unloaded) microbubbles.

I. INTRODUCTION

Image guided ultrasound-targeted drug delivery using liposome-loaded microbubbles could become a new approach for cancer treatment [1], as the toxic chemotherapy agents can be encapsulated and released locally upon the proper stimuli (such as high intensity ultrasound). This has significant potential for reduction in side effects compared with a systematic delivery. A key component of this approach is the ability to track these drug vehicles in real time to guide payload release upon their arrival at the desired location. The imaging capability of these drug-loaded microbubbles could be further explored as a biomarker for the treatment response or a tool for drug dose estimation for personalized medicine [2]. Microbubble detection techniques with high sensitivity and less disruption are thus highly preferable for these applications.

The subharmonic emission, with respect to second harmonic and other superharmonic emissions, is exclusive to microbubbles at diagnostic pressure levels [3]. The potential use of microbubble subharmonic signals has been demonstrated by a range of studies, such as non-invasive blood pressure estimation [4], quantification of perfusion [5], molecular imaging [6] and 3D ultrasound imaging [7], among others. However, the subharmonic nonlinearity of microbubbles only occurs when an acoustic pressure threshold is exceeded [3]. Buckling the microbubble lipid shell gives rise to the reduced acoustic pressure threshold for the initiation of subharmonics [8]. For bare phospholipid-coated microbubbles, gas diffusion from the core into the surrounding liquid could account for shell buckling and microbubbles can be compressed but hard to expand in rarefaction phases (‘compression-only’ behaviour). With attachment of drug filled liposomes to the microbubble shell, ultrahigh-speed optical imaging revealed an ‘expansion-only’ microbubble behaviour, which mostly happened at low

pressures (< 30 kPa) [9]. In response to the incident acoustic field, liposome-loaded microbubbles undergo expansion, but very limited compression. More recently, acoustic characterization of liposome-loaded microbubble populations confirmed the subharmonic emissions at low pressures (< 50 kPa) [10]. It is hypothesized that the decreased threshold for the generation of subharmonic emissions is related to the ‘expansion-only’ behaviour whereby microbubbles are enforced to a buckled state by the packed liposome layer.

The lower subharmonic threshold for the liposome-loaded microbubbles could be most beneficial for high frame-rate imaging by transmitting plane waves, whereby the imaging depth is currently limited by the lack of transmission focus. The use of plane wave contrast imaging has enabled the continuous monitoring of microbubbles with improved contrast [11], [12]. As opposed to the line-by-line imaging mode, plane wave imaging (PWI) spreads the spatial peak acoustic intensity over multi-pulses to preserve the survival rate of microbubbles, as the mechanical index (MI) will be the key determinant for microbubble destruction.

As unique signals from microbubbles, the subharmonic emissions are of interest to provide consistent contrast response. The aim of this study was to investigate whether the lowered acoustic pressure threshold for the production of subharmonics from liposome-loaded microbubbles could improve their ability to perform subharmonic PWI.

II. MATERIALS AND METHODS

A. *Manufacture of Liposomes and Microbubbles*

Liposomes encapsulating propidium iodide were manufactured prior to loading them to microbubbles [13]. The phospholipids used for liposomes were prepared by mixing DSPC, cholesterol and DSPE-PEG2000-Biotin (all from Avanti Polar Lipids, Alabaster, AL, USA) dissolved in chloroform with a molar fraction 62.8%, 32.3% and 4.8%, respectively. Drying chloroform was performed in vacuum for 24 hours. The dried lipid film was then hydrated by addition of 500 μ L buffer comprising 1 mg/mL propidium iodide (P4864, Sigma-Aldrich, Dorset, UK). The solution was vortex mixed until all lipids dissolved into it. Liposomes were made by repeatedly extruding the prepared solution through a mini-extruder (Avanti Polar Lipids, Alabama, United States) that was heated to 60°C on a hot plate. To remove excess propidium iodide, the solution

was passed through a column (G-25, GE Healthcare, Buckinghamshire, United Kingdom). Liposomes with a mean diameter of 200 nm were finally manufactured with a concentration of 1×10^{13} liposomes/ml.

Unloaded microbubbles were prepared by mixing 84 μL DPPC and 14 μL DSPE-PEG2000-Biotin with a concentration of 20 mg/mL (Avanti Polar Lipids, Alabaster, AL, USA) [13]. After the stock chloroform was evacuated in a vacuum desiccator for 24 hours, the dried lipids were re-suspended in 1 mL buffer containing 99% purified water and 1% glycerine (by volume) and 4 mg/mL NaCl in a 1 mL vial. The vial was vortexed for 45 seconds before placed in an ultrasound bath (U50, Ultrawave Ltd., Cardiff, UK) for 15 minutes to facilitate the lipid re-suspension. Finally, microbubbles were produced by saturating the prepared lipid solution with perfluorobutane (C_4F_{10}) followed by 15-second shaking using a CapMix mechanical shaker (ESPE, 3M Co., St. Paul, MN).

For liposome-loaded microbubbles, a 200 μL liposome solution was added with 10 μL of NeutrAvidin (A2666, Invitrogen Life Technologies, Paisley, UK), followed by incubation for 20 minutes at room temperature. The liposome solution was then added to a 1 mL unloaded microbubble solution and further incubated for 20 minutes at room temperature to form liposome-loaded microbubbles by linking liposomes to the microbubble shell through biotin-neutravidin binding.

Both types of microbubbles were optically inspected and analyzed using an inverted microscope (Eclipse Ti-U, Nikon Instruments Inc., Tokyo, Japan) [14] to determine the microbubble concentration and size distribution. Unloaded and liposome-loaded microbubbles showed similar concentrations containing the order of 1×10^{10} microbubbles/mL. In all experiments, microbubble solutions were diluted with purified water and a concentration of 1.9×10^6 microbubbles/mL was used. A mean diameter of $1.6 \pm 0.9 \mu\text{m}$ and $1.6 \pm 0.8 \mu\text{m}$ was found for unloaded microbubbles and liposome-loaded microbubbles, respectively.

B. Subharmonic Imaging Setup and Ultrasound Parameters

A tissue mimicking material (TMM) wall-less flow phantom [15] was fabricated for the experimental component of this study. A 2.8-mm flow channel was embedded with an oblique angle relative to the transducer-phantom interface. The average attenuation and speed of sound through this TMM was measured to be $0.3 \text{ dB}\cdot\text{cm}^{-1}\cdot\text{MHz}^{-1}$ and 1547 m/s, respectively.

Microbubble solutions with a concentration of 1.9×10^6 microbubbles/mL were continuously stirred and allowed to homogenize for 20 seconds prior to each measurement. The inlet of the flow channel was connected to a syringe through tubing. The prepared microbubble solutions were pumped through the channel with a mean flow velocity of 20 mm/s.

The Ultrasound Array Research Platform II (UARP II) [16] equipped with a Verasonics L11-4 probe was used to generate subharmonic PWI. The transducer had a -6 dB bandwidth of 90.8% and a center frequency at 7.55 MHz. Peak negative pressures (PNPs) were measured in water with a 200 μm

calibrated needle hydrophone (Precision Acoustics, Dorchester, UK) to determine the *in situ* MI of 0.09. A pulse sequence of 15 plane waves (6-cycle 9 MHz), steered from -5° to 5° with an even angle step, was emitted with a pulse repetition frequency (PRF) of 6 kHz. Each pulse sequence was separated by a 2-second period, to transfer the RAW data to the local drive and also allow for replenishment of microbubble populations between two acquisitions. Each measurement comprised of 10 transmissions of the sequence and the measurement was repeated for three times. Prior to each measurement, the flow tunnel was thoroughly rinsed with water. Subharmonic PWI was performed with both types of microbubbles for comparison.

The downloaded channel data was reconstructed offline by delay-and-sum beamforming in Matlab (The MathWorks, Natick, MA, USA). For subharmonic PWI, the echoes from 15 angled plane waves were coherently summed to retrieve one compounded frame. The RF beamformed data was then filtered using a bandpass filter (3 - 4.5 MHz). The filtered data was then Hilbert transformed and the enveloped data was used to calculate the subharmonic amplitude in ROIs as shown in Fig. 1 (a).

III. RESULTS

Fig. 1 shows, from left to right, typical frames acquired for fundamental PWI with water only, subharmonic PWI with unloaded and liposome-loaded microbubbles, respectively. Two ROIs of A and B were delimited by green and red lines as shown in Fig. 1 (a) and corresponding subharmonic amplitudes for both types of microbubbles are given in Fig. 2. Fig. 1 (b) shows that the subharmonic signals from unloaded microbubbles diminish with depth. For subharmonic PWI, Fig. 2 shows that the average subharmonic intensity in ROI B is higher with liposome-loaded microbubbles, and the intensity difference with these two types of microbubble populations has been significantly larger in ROI A. These occurred as a result of the lack transmission focus with plane waves. The acoustic pressure was gradually attenuated with depth and lower than the threshold to elicit subharmonic responses for unloaded microbubbles. However, for liposome-loaded microbubbles, subharmonic nonlinearity sets in with a reduced acoustic pressure threshold, and this enables higher subharmonic sensitivity particularly at deep locations as shown in Fig. 1 (c).

IV. DISCUSSION

The effects of the number of liposomes linked to the microbubble on subharmonic emissions need to be explored in the future. Long-duration coded excitations such as chirps could be used to substantially increase the subharmonic generation [17]. However, with chirps the axial resolution can be only partially preserved on the receiving side mainly because of phase variations due to microbubble vibration and destruction, creating one of the worst scenarios for pulse compression [18].

Generally, the pressure threshold for subharmonic emissions could be minimized when microbubble populations are driven

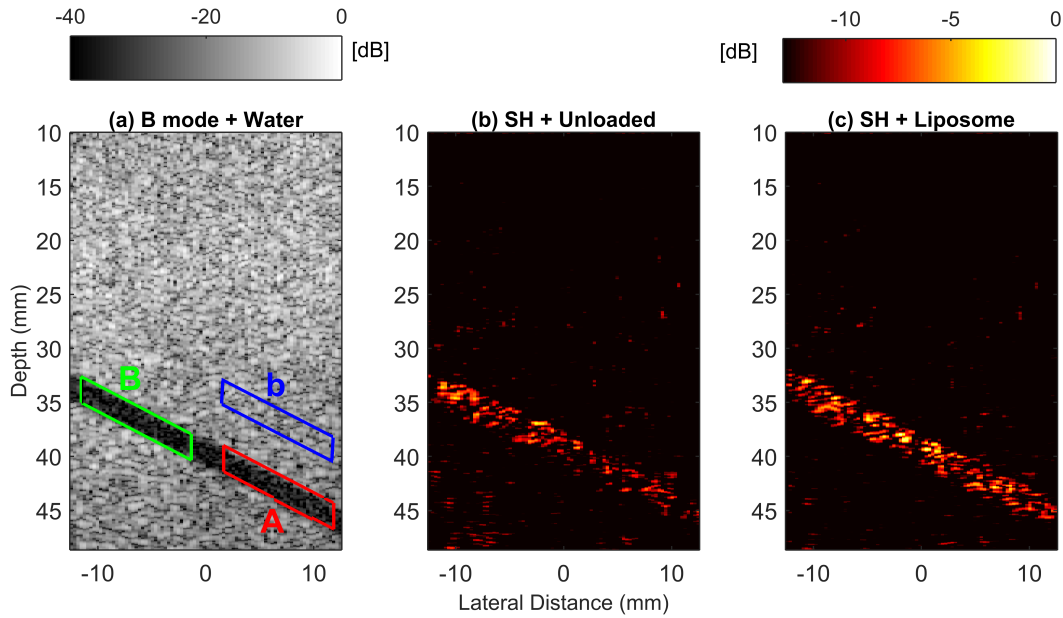


Fig. 1. (a) B-mode image showing ROIs. Subharmonic images with (b) unloaded microbubbles and (c) liposome-loaded microbubbles. SH: subharmonic.

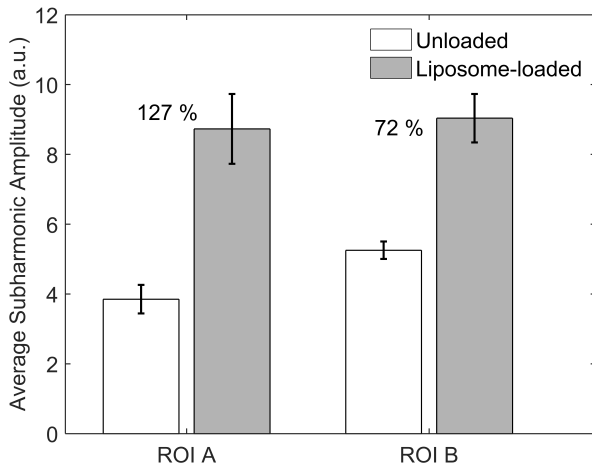


Fig. 2. The average subharmonic amplitude and relative amplitude difference in percentage for ROI A and ROI B (results based on $10 \times 3 = 30$ measurements).

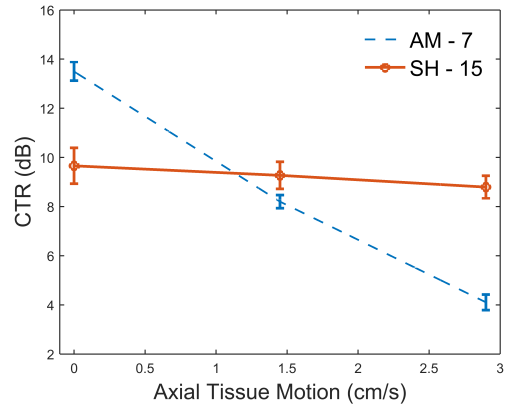


Fig. 3. Effects of tissue motion on CTR for AM and subharmonic PWI. The numbers of 7 and 15 indicate the number of steering angles for compounding.

at twice of their resonance frequency. Acoustic characterisation of the microbubble populations could hence benefit subharmonic imaging when providing the accurate resonance frequency.

A lot of techniques, such as amplitude modulation (AM) and pulse inversion (PI) [19], exist in commercial systems for contrast-enhanced imaging through exploiting non-linear fundamental and second harmonic oscillations of microbubbles. Whereas the use of PI and AM could provide an improvement of contrast, the nature of non-linear wave propagation hampers their ability to discriminate microbubbles and tissue. Additionally, tissue motion results in decorrelation of tissue signals within the PI or AM packet, leaving residual signals

but misclassified as contrast [12]. The influence of tissue motion on the contrast-to-tissue ratio (CTR) with liposome-loaded microbubbles, if any, was investigated through artificially displacing the raw channel data with subharmonic PWI [20]. The tissue motion of 1.4 or 2.8 cm/s was simulated in the direction of ultrasound propagation. For comparison, amplitude modulation (AM) PWI with a 2-pulse packet was designed. The excitation signal was a 3-cycle 4.5 MHz sinusoid tapered with a Tukey window (coefficient: 0.2). The same PRF of 6 kHz, MI of 0.09 and the 10° sector angle as those employed for subharmonic PWI were used. But the number of scanning angles was reduced to 7 in one pulse sequence. This configuration was determined so that the imaging time for a final compound image was comparable to that for subharmonic PWI. Fig. 3 shows the CTR measurements between ROIs B

and b with varied artificial tissue speeds. For AM, the CTR is significantly susceptible to tissue motion, while this is not the case for subharmonic PWI. This might suggest that when using plane waves, subharmonic imaging is more suitable for the quantitative applications of microbubbles, such as perfusion imaging and quantification of liposome-loaded microbubbles.

V. CONCLUSIONS

The present study experimentally demonstrated subharmonic PWI of liposome-loaded microbubbles with improved sensitivity compared to that with unloaded microbubbles. This could be explained by that liposome-loaded microbubbles are able to generate subharmonics at a reduced pressure threshold, through naturally forcing bubbles to the buckling state by the loaded liposome layer. This technique could be used for specifically tracking payload loaded on microbubbles and has the potential for drug volume estimation.

VI. ACKNOWLEDGEMENT

This work was supported by the EPSRC under Grant EP/P023266/1 and EP/N034813/1. J. R. McLaughlan would like to acknowledge support from an EPSRC Innovation Fellowship EP/S001069/1.

REFERENCES

- [1] J. Escoffre, C. Mannaris, B. Geers, A. Novell, I. Lentacker, M. Averkiou, and A. Bouakaz, "Doxorubicin liposome-loaded microbubbles for contrast imaging and ultrasound-triggered drug delivery," *IEEE Transactions on Ultrasonics, Ferroelectrics, and Frequency Control*, vol. 60, no. 1, pp. 78–87, January 2013.
- [2] J. M. Hudson, R. Williams, C. Tremblay-Darveau, P. S. Sheeran, L. Milot, G. A. Bjarnason, and P. N. Burns, "Dynamic contrast enhanced ultrasound for therapy monitoring," *European Journal of Radiology*, vol. 84, no. 9, pp. 1650–1657, 2015.
- [3] W. Shi, F. Forsberg, J. Raichlen, L. Needleman, and B. Goldberg, "Pressure dependence of subharmonic signals from contrast microbubbles," *Ultrasound in Medicine & Biology*, vol. 25, no. 2, pp. 275–283, 1999.
- [4] J. K. Dave, S. V. Kulkarni, P. P. Pangaonkar, M. Stanczak, M. E. McDonald, I. S. Cohen, P. Mehrotra, M. P. Savage, P. Walinsky, N. J. Ruggiero II *et al.*, "Non-invasive intra-cardiac pressure measurements using subharmonic-aided pressure estimation: Proof of concept in humans," *Ultrasound in Medicine & Biology*, vol. 43, no. 11, pp. 2718–2724, 2017.
- [5] F. Forsberg, J.-B. Liu, W. T. Shi, R. Ro, K. J. Lipcan, X. Deng, and A. L. Hall, "In vivo perfusion estimation using subharmonic contrast microbubble signals," *Journal of Ultrasound in Medicine*, vol. 25, no. 1, pp. 15–21, 2006.
- [6] R. Gessner and P. A. Dayton, "Advances in molecular imaging with ultrasound," *Molecular Imaging*, vol. 9, no. 3, pp. 7290–2010, 2010.
- [7] J. R. Eisenbrey, A. Sridharan, P. Machado, H. Zhao, V. G. Halldorsdottir, J. K. Dave, J.-B. Liu, S. Park, S. Dianis, K. Wallace *et al.*, "Three-dimensional subharmonic ultrasound imaging in vitro and in vivo," *Academic Radiology*, vol. 19, no. 6, pp. 732–739, 2012.
- [8] N. De Jong, M. Emmer, C. T. Chin, A. Bouakaz, F. Mastik, D. Lohse, and M. Versluis, "compression-only behavior of phospholipid-coated contrast bubbles," *Ultrasound in Medicine & Biology*, vol. 33, no. 4, pp. 653–656, 2007.
- [9] Y. Luan, T. Faez, E. Gelderblom, I. Skachkov, B. Geers, I. Lentacker, T. van der Steen, M. Versluis, and N. de Jong, "Acoustical properties of individual liposome-loaded microbubbles," *Ultrasound in Medicine & Biology*, vol. 38, no. 12, pp. 2174–2185, 2012.
- [10] J. R. McLaughlan, S. Harput, R. H. Abou-Saleh, S. A. Peyman, S. Evans, and S. Freear, "Characterisation of liposome-loaded microbubble populations for subharmonic imaging," *Ultrasound in Medicine & Biology*, vol. 43, no. 1, pp. 346–356, 2017.
- [11] O. Couture, M. Fink, and M. Tanter, "Ultrasound contrast plane wave imaging," *IEEE Transactions on Ultrasonics, Ferroelectrics, and Frequency Control*, vol. 59, no. 12, pp. 2676–2683, Dec 2012.
- [12] J. Viti, H. J. Vos, N. d. Jong, F. Guidi, and P. Tortoli, "Detection of contrast agents: Plane wave versus focused transmission," *IEEE Transactions on Ultrasonics, Ferroelectrics, and Frequency Control*, vol. 63, no. 2, pp. 203–211, Feb 2016.
- [13] S. A. Peyman, R. H. Abou-Saleh, J. R. McLaughlan, N. Ingram, B. R. Johnson, K. Critchley, S. Freear, J. A. Evans, A. F. Markham, P. L. Coletta *et al.*, "Expanding 3d geometry for enhanced on-chip microbubble production and single step formation of liposome modified microbubbles," *Lab on a Chip*, vol. 12, no. 21, pp. 4544–4552, 2012.
- [14] J. McLaughlan, N. Ingram, P. R. Smith, S. Harput, P. L. Coletta, S. Evans, and S. Freear, "Increasing the sonoporation efficiency of targeted polydisperse microbubble populations using chirp excitation," *IEEE transactions on ultrasonics, ferroelectrics, and frequency control*, vol. 60, no. 12, pp. 2511–2520, 2013.
- [15] L. Nie, S. Harput, D. M. J. Cowell, T. M. Carpenter, J. R. McLaughlan, and S. Freear, "Combining acoustic trapping with plane wave imaging for localized microbubble accumulation in large vessels," *IEEE Transactions on Ultrasonics, Ferroelectrics, and Frequency Control*, vol. 65, no. 7, pp. 1193–1204, July 2018.
- [16] E. Boni, A. C. H. Yu, S. Freear, J. A. Jensen, and P. Tortoli, "Ultrasound open platforms for next-generation imaging technique development," *IEEE Transactions on Ultrasonics, Ferroelectrics, and Frequency Control*, vol. 65, no. 7, pp. 1078–1092, July 2018.
- [17] S. Harput, M. Arif, J. McLaughlan, D. M. J. Cowell, and S. Freear, "The effect of amplitude modulation on subharmonic imaging with chirp excitation," *IEEE Transactions on Ultrasonics, Ferroelectrics, and Frequency Control*, vol. 60, no. 12, pp. 2532–2544, Dec 2013.
- [18] S. Harput, J. McLaughlan, D. M. J. Cowell, and S. Freear, "Contrast-enhanced ultrasound imaging with chirps: Signal processing and pulse compression," in *2015 IEEE International Ultrasonics Symposium (IUS)*, Oct 2015, pp. 1–4.
- [19] R. J. Eckersley, C. T. Chin, and P. N. Burns, "Optimising phase and amplitude modulation schemes for imaging microbubble contrast agents at low acoustic power," *Ultrasound in Medicine & Biology*, vol. 31, no. 2, pp. 213–219, 2005.
- [20] P. Gong, P. Song, and S. Chen, "Improved contrast-enhanced ultrasound imaging with multiplane-wave imaging," *IEEE Transactions on Ultrasonics, Ferroelectrics, and Frequency Control*, vol. 65, no. 2, pp. 178–187, Feb 2018.